Investigation of turbulent separation in a forward-facing step flow

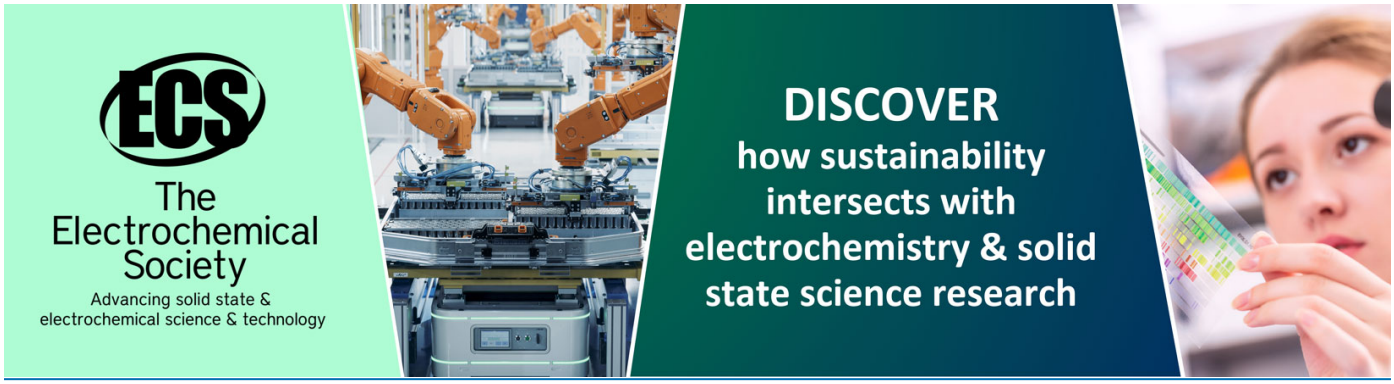

Journal of Physics: Conference Series **318** (2011) 022031 doi:10.1088/1742-6596/318/2/022031

Investigation of turbulent separation in a forward-facing step flow

D S Pearson[1], P J Goulart[1,2] and B Ganapathisubramani[1,3]

[1] Department of Aeronautics, Imperial College London, UK.
[2] Automatic Control Laboratory, ETH Zürich, Switzerland.
[3] School of Engineering Sciences, University of Southampton, UK.

E-mail: d.pearson08@imperial.ac.uk

Abstract.

The relation between the upstream and downstream regions of separation of the flow over a forward-facing step is investigated using experimental data. High-speed Particle Image Velocimetry (PIV) data is used to show a correlation between the wall shear stress of the oncoming boundary layer and the streamwise location of reverse flow upstream of the step. The time delay associated with the correlation is consistent with average convection velocities in the lower boundary layer. This suggests that appropriate addition of momentum into the boundary layer could be used to control the spatial extent of the separation upstream of the step.

In addition, low-speed PIV data is used to show statistical relations between the flow characteristics of the recirculation regions in the vicinity of the step face. It is shown that a slower than average flow velocity above the step face is associated with an increase in the wall-normal extent of upstream reverse flow, an increase in the inclination of the flow above the step and an increase in downstream vorticity.

1. Introduction

The flow over a forward-facing step submerged in a turbulent boundary layer produces complex flow structures for which the local dynamic mechanisms remain largely unexplained. It is a canonical configuration with significance to both fundamental fluid dynamics research and applied engineering design. Despite this however, it has been the subject of far fewer investigations relative to those of a backward facing-step (Sherry *et al.*, 2009).

The complexity of the flow is due to the presence of two regions of separation, each formed under different flow conditions. The upstream separation arises from the adverse pressure gradient caused by the blockage of flow at the step face. This separation is therefore bounded on two sides while being exposed to the momentum of oncoming turbulent boundary layer. The downstream separation is caused by the flow over a sharp edge and therefore has a fixed point of separation. The motions of this region are predominantly characterised by the shedding of vortices from the step corner and their convection downstream (Kiya & Sasaki, 1983).

The recirculation within the upstream separation is frequently three-dimensional. In laminar flow, Stüer *et al.* (1999) attribute this to the entrainment of fluid from the oncoming boundary layer causing the upstream vortex to become unstable. Such instabilities often result in flow passing up and over the face of the step and interacting with the separation bubble above.

It is the downstream separation bubble which often proves most problematic from an engineering design point of view, since this is the region of highest static pressure fluctuations (Camussi *et al.*, 2008; Largeau & Moriniere, 2007) and is therefore likely to be the highest source of noise and viscous drag from this flow regime. If the origins of these fluctuations can be traced upstream, past the step face, this would open up possibilities to control of downstream noise and drag through manipulation of the oncoming boundary layer.

For this to be achievable, knowledge is required of the interactions between the turbulent boundary layer, the recirculation upstream of the step face, and the shedding of vortices from the step corner. This study uses Particle Image Velocimetry (PIV) to investigate the statistical relationship between several defined flow parameters at the step face. The dependence of these parameters on the upstream and downstream flows is then investigated using time-resolved PIV data and a sequence of events leading to reduced levels of downstream turbulence is suggested.

2. Experimental setup

A step of height h=0.03m was placed into the turbulent boundary layer of a wind tunnel with cross section 1.37m×1.12m. The boundary layer was tripped using a surface roughness 1.90m upstream of the step, producing a boundary layer displacement thickness of $\delta_{\text{no step}}$=0.049m at a free stream velocity of 10ms^{-1}. The step is therefore wholly submerged in the boundary layer, with δ/h=1.63 and the Reynolds number based on step height of $Re_h = U_\infty h/\nu = 20.5 \times 10^3$. The step spanned the entire width of the tunnel and continued over $30h$ downstream.

2.1. PIV measurements

In this study, data from two Particle Image Velocimetry (PIV) experiments are used to investigate the dependencies of the downstream separation to the upstream flow patterns. The first data set consists of 1500 two-dimensional vector fields taken using a low-speed PIV system. The interrogation area was illuminated using a Litron nano PIV 200mJ/pulse Nd:Yag laser and the images were captured with two TSI Powerview Plus cameras. The cameras had 2048×2048 pixel CCDs and were fitted with a Nikon 105mm lens. The vector fields were acquired at a rate of 1Hz using pairs of images $dt = 45\mu s$ apart. The relatively low dt value was required to resolve sufficiently the high shear gradients produced by the downstream separation. The vectors were processed using a recursive algorithm from a 128×128 pixel to a 16×16 pixel interrogation window with 50% overlap. This provided velocity vectors with approximately 0.4mm spacing, equivalent to $h/75$. An example vector field from this data set is shown in Figure 1(a). The vector field color scale is normalised by the free stream velocity and the coordinates are normalised by the step height h. The flow is from left to right.

The second data set consists of 8000 image pairs taken over 4 seconds at a rate of 2000Hz. This data set provides a time-resolved measurement of the flow, enabling the evolution of the flow structures to be studied. The high-speed PIV system consisted of a 20mJ/pulse Nd:YLF laser with a Phantom V12 CMOS camera with 800×1280 pixels and a Sigma EX Macro 150mm lens. The images were taken 75μs apart and were processed using the same software algorithms as those used on for low speed data, producing velocity vectors with 1.1mm spacing ($h/27$). The field of view and spatial resolution of the vectors can be seen from Figure 1(b). The Figures 1(a) and 1(b) are shown at the same scale.

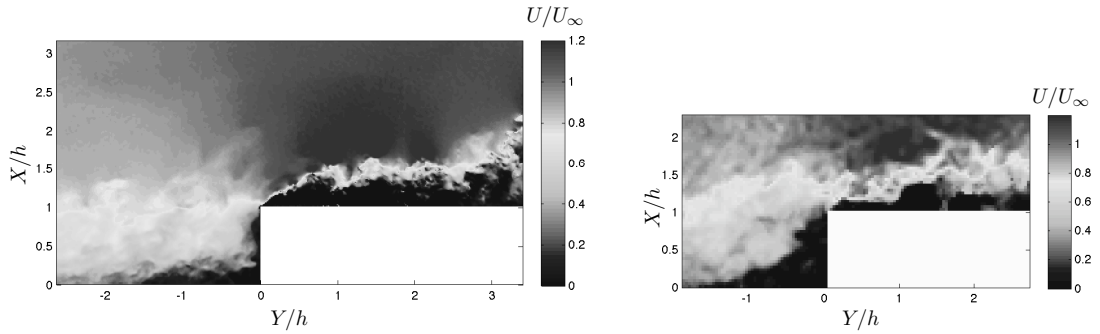

Figure 1. Example vector fields from PIV data sets used. a) Low speed data, b) High speed data.

3. Results

For both the low-speed and high-speed data, a number of flow-field parameters are calculated from each vector field. The relative location of each parameter is shown schematically in Figure 2. The distribution of values for each parameter relative to another provides the basis of the following analyses.

The parameters can be broadly grouped into three categories. Those upstream of the step, those in the vicinity of the step, and those downstream. The upstream flow parameters are the wall shear stress, τ_w, and the boundary layer displacement thickness, δ^*, defined by

$$\tau_w = \left.\frac{\partial U}{\partial y}\right|_{y=0}$$
$$\delta^* = \int_0^\infty \left(1 - \frac{U}{U_\infty}\right) dy,$$

respectively. U_∞ is the free stream velocity and y is the wall-normal direction. These two quantities are inherently linked by the distribution $\partial U/\partial y$, with δ^* providing a measure of mass flow deficit due to the presence of the boundary layer, and τ_w the velocity gradient very close to the wall. In this study τ_w is calculated over the first two vectors in y ($\Delta y \approx 1.1$mm) over the streamwise extent shown in Figure 2, and serves only as an approximation to the actual wall shear stress.

The parameters in the vicinity of the step are the boundary layer displacement thickness at the step edge δ^*_{step}, and the magnitude and angle of the flow above the step corner coordinate $(0, 1.1h)$, labelled $|U|_2^c$ and α^c respectively. Also recorded are approximations to the spatial limits of the upstream separation region, X^+ and Y^+. The spatial limits of separation are not easily discernible for an instantaneous image of turbulent flow; the streamline contours are complex and meandering. Instead, the spatial distribution of vectors with velocity $U < 0$ was taken as an approximation, for example Y^+ is the largest Y coordinate of all vectors with $U < 0$ upstream of the step. Such vectors provide a conservative estimate of separation size, since in this flow configuration they only occur within the boundaries of a separation bubble.

The flow downstream of the step has been partitioned into regions labelled **A** to **E**, each of width $\Delta X/h = 0.5$. For each region the mean spanwise vorticity ω_z and the centroid of the vectors with negative streamwise velocity $(\bar{X}, \bar{Y})$ was calculated.

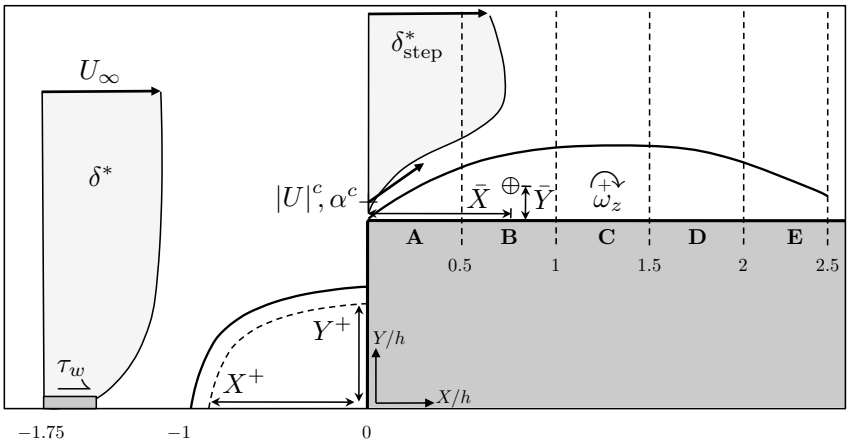

Figure 2. Schematic diagram of the different parameters studied.

4. Analysis and discussion

4.1. Flow in the vicinity of the step

In order to examine the relationship between the different above-mention parameters, the Joint Probability Density Function (joint-pdf) has been computed. Figure 3 shows the joint-pdf of four parameter pairings for the low-speed PIV data. The contours show lines of equal probability density and the colour scale is normalised such that the volume enclosed by the contours, i.e. the probability of all events, is equal to unity. Two statistically independent variables would have a joint-pdf with two lines of symmetry parallel to the chart axes. This would show that for any change in the first variable there is equal probability the second variable lies either side of its mean. Two variables with a strong linear correlation would appear as a straight and narrow contour ridge inclined to the chart axes. To aid clarity, each figure is shown with lines of the mean and $\pm 1, 2$ standard deviations, for both abscissa and ordinate.

Figures 3(a) and 3(b) show how the two separation regions, upstream and downstream, move within the flow. The negative trend of Figure 3(a) indicates a strong tendency of the upstream bubble to grow in both -X and +Y directions simultaneously, i.e. it expands and contracts from the lower corner of the step by which it is bounded. On expansion, the maximum vertical extent of reverse flow is roughly equal to the height of the step. During such events, the separation bubble must also necessarily be at least the height of the step. This implies that in rare cases mass flow could occur between the upper and lower step surfaces. The likelihood of such cases is consistent with a positive two standard deviation event in Y^+.

In contrast, Figure 3(b) indicates the centroid of the downstream separation region has a tendency to move downstream as it rises. This is intuitively consistent with a separation bubble with a fixed point of separation being buffeting by oncoming flow. It is likely this movement is coupled to the tendency shown in Figure 3(c) with shows the measurements of magnitude and angle of the velocity vector at the step corner. The clear negative relation between the velocity magnitude and angle relative to free stream demonstrates that the flow tends to be faster when the angle is closer to horizontal, and slower when at larger upward angles. The change in corner flow speed at different angles could go some way toward explaining movement of the downstream bubble in Figure 3(b). Likewise, the change in corner flow speed would be expected to have a direct influence on the local boundary layer displacement thickness at the step corner, since this is the integral over y of all velocities at this location.

The displacement thickness is shown in Figure 3(d) in relation to the upstream wall-normal extent of negative flow. The notable feature of this figure is the weak relation between the two

quantities (indicated by the near-vertical apex of the contours) until the largest wall-normal extent of reverse flow nears the height of the step. Such events occur with a deficit of flow momentum (high displacement thickness) over the step corner. A plausible link between these four figures is the simultaneous occurrence of a large upstream separation bubble, with high corner displacement thickness, and a low corner velocity at a high angle. This would create the conditions suited to a large upstream separation with a high centroid of reverse flow.

Despite the intuitive mechanical link between the parameters shown in Figures 3(a) to 3(d), the low-speed PIV joint-pdf relations only show the likelihood of joint occurrence of events and cannot offer evidence of the cause and effect between parameters. However, this information can be obtained by cross-correlating the time history of the parameters from the high-speed PIV data, since time delays in the cross correlation indicate precedence.

The cross correlations corresponding to joint-pdf Figures 3(a) to 3(d) are shown in Figures 4(a) to 4(d). These correlations, shown as a function of time delay, confirm that these four relations have Δt at or near zero and hence occur simultaneously. Any temporal dependence between these parameters either occurs at speeds greater than the PIV sample rate or has been lost during the averaging necessary for PIV post processing. However, this result does confirm that the use of low-speed PIV is valid for joint-pdfs of parameters within close proximity in this configuration.

4.2. Correlation with the upstream flow

Extending the use of cross correlations to the upstream parameters δ^* and τ_w allows dependencies with the oncoming flow to be found. The correlation between the upstream displacement thickness and the step displacement thickness is shown in Figure 5(a), and that of the wall shear stress and the location of most upstream reverse flow in 5(b). The x-scale of these two figures is the correlation time delay non-dimensionalised using the free stream velocity and step height. Inspection of the peaks shows non-dimensional delays of 2.33 and 2.17, which for this experiment correspond to delays of 7ms and 6.5ms respectively. This means that on average the displacement thickness at the step bears most resemblance to what the upstream displacement thickness was 7ms previously, and similarly for the relation between the upstream extent of reverse flow and the wall shear stress.

The delay show in Figure 5(a) with a separation between the stations of $X = 1.75h$ corresponds to an average convection velocity of $U/U_\infty = 0.75$. This convection speed is consistent with the mean velocity of a mid-boundary layer region. Likewise for the parameters in Figure 5(b) with spatial separation of $X \approx 0.75h$, the non-dimensional time delay of 2.17 corresponds to an average convection velocity of $U/U_\infty = 0.35$, which is consistent with boundary layer speeds very close to the wall.

The direction of the correlations in Figures 5 is also of note. A low displacement thickness (increased velocity) in the upstream boundary layer is strongly correlated to a low displacement thickness over the step. Also, a high upstream shear stress (increased velocity) is correlated to a positive movement (toward the step) of the streamwise extent of the reverse flow. These results show that the a high velocity motion of the upstream boundary layer simultaneously suppresses the separation region upstream of the step and increases the flow velocity over the step. It is therefore reasonable to postulate that the shape of the upstream separation bubble is not only dependent on δ/h and $\mathrm{Re_h}$ as noted by Sherry *et al.* (2009), but also on $\partial U/\partial y$; the profile of the oncoming boundary layer.

Using the cross correlation time delays from Figures 5, the joint-pdf can be viewed with the appropriate delay incorporated, thereby ensuring the strongest trends are shown. These joint-pdfs are shown in Figures 6. They show a strong positive-trend between the upstream and step displacement thicknesses (Figure 6(a)), and also a clear tendency for low upstream wall shear to allow the upstream separation to advance further upstream (Figure 6(b)).

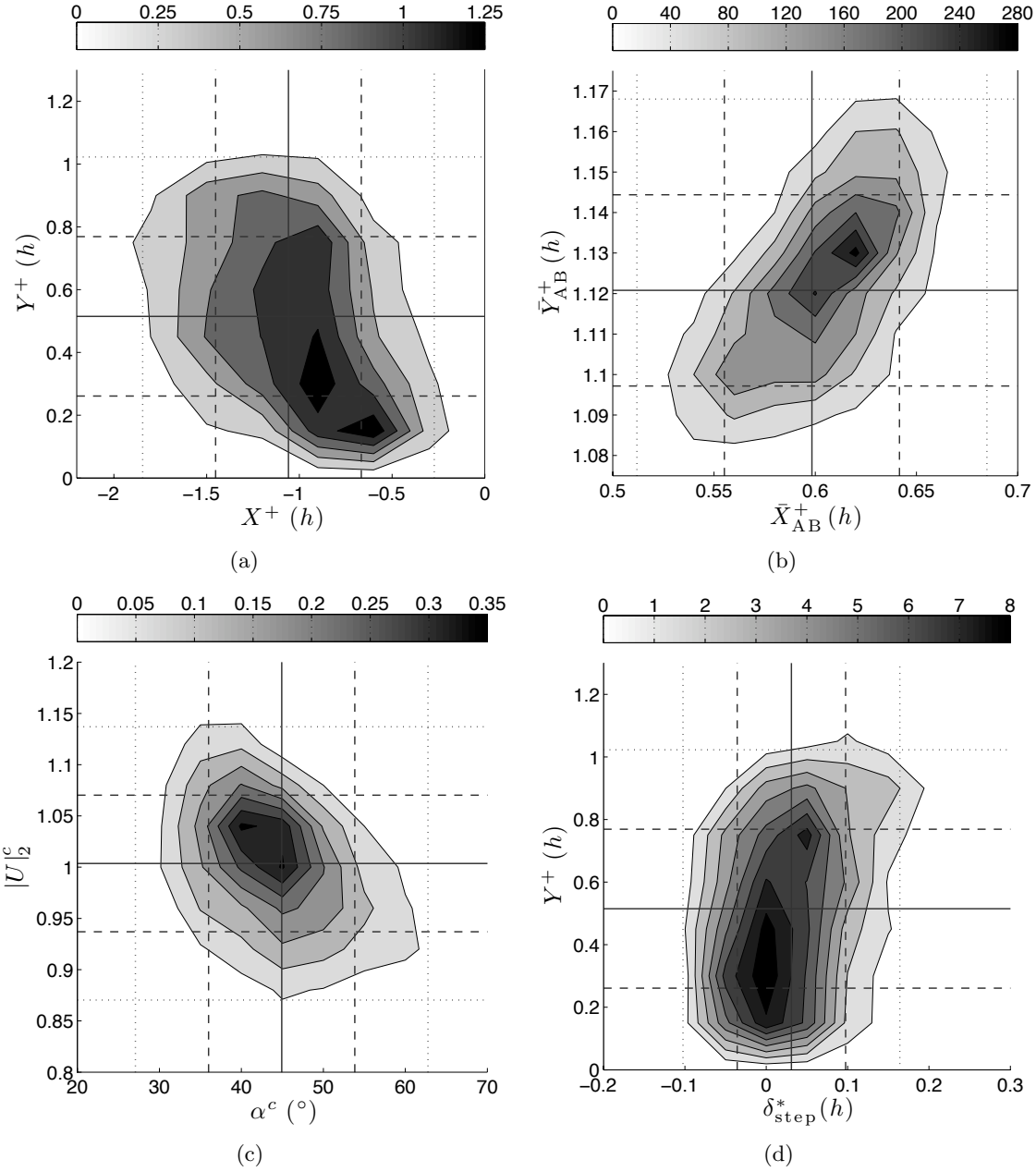

Figure 3. Joint probability density functions for selected parameters using low-speed PIV data. Contour colour scales are normalised such that the bounded volume is unity.
Parameter symbols are defined in Figure 2.

——— abscissa mean, ordinate mean
- - - - - - abscissa ±1std, ordinate ±1std
····· abscissa ±2std, ordinate ±2std

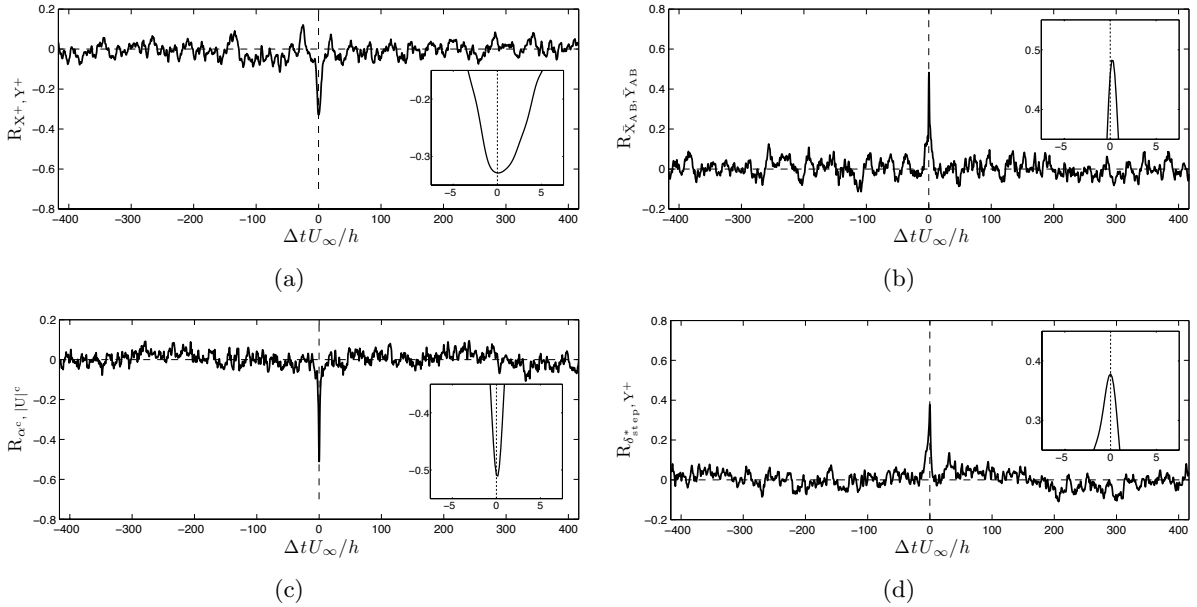

Figure 4. Cross correlations of parameter pairs corresponding to charts a) to d) in Figure 3. All correlation peaks show no appreciable time delay.

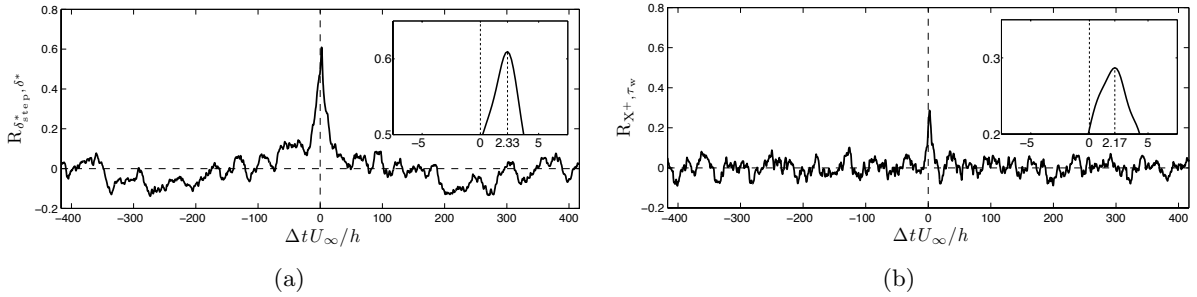

Figure 5. Cross correlations of parameter pairs: a) δ^*_{step} and δ^*, b) X^+ and τ_w

4.3. Correlation with the downstream flow

The form of the separation downstream of the step is difficult to quantify, except in the mean. Compared to the upstream separation, the magnitude of turbulent fluctuations is higher and the spatial extent of the separation is greater. Another notable feature of downstream separation are the increased levels of vorticity. Figure 7 shows that the mean vorticity in region **A** has a strong negative correlation with the displacement thickness at the step – a high displacement thickness (low momentum flow) increases the mean vorticity at station **A** with approximately zero time delay.

Sigurdson (1995) attributes the production of vortices to two mechanisms. Firstly, those created by shedding from the step corner, and secondly those arising from to Kelvin-Helmholtz instabilities within the free shear layer. Similar conclusions were made by Kiya & Sasaki (1983) in which they associate the latter with a 'flapping' motion of the shear layer at the point of separation. The present results support this observation, namely a strong link between a high displacement thickness with a more inclined angle of flow at the step corner (Section 4.1) and with an increased level of mean vorticity near the step (Figure 7(b)).

That the vortex production can be linked to the step displacement thickness and corner

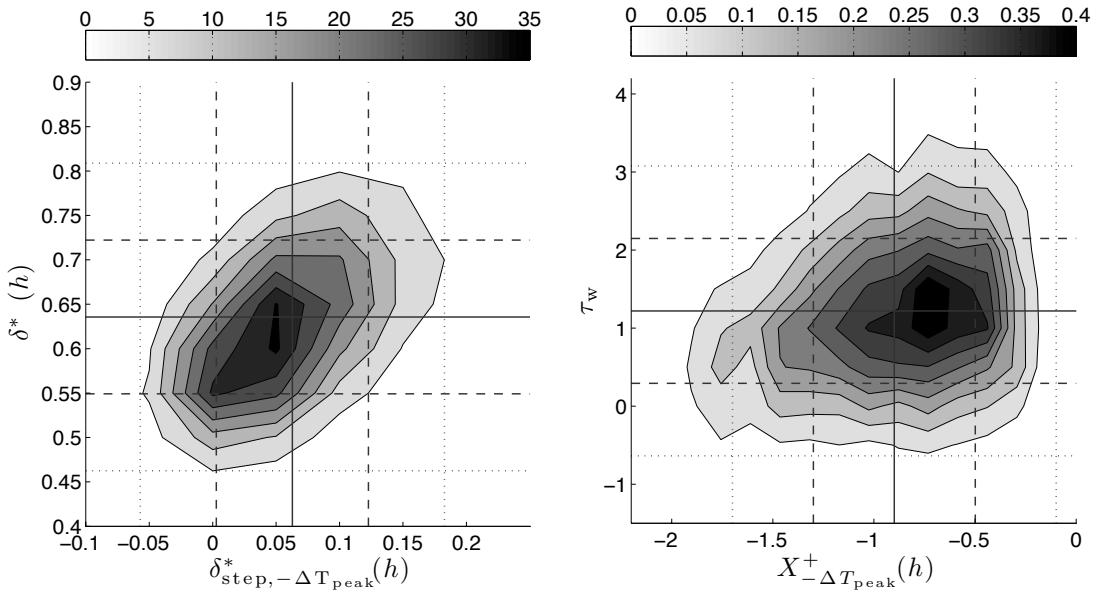

Figure 6. Joint probability density functions corresponding to parameters in Figure 5, taken from high-speed PIV data with Δt offset. Contour colour scales are normalised such that the bounded volume is unity. Parameter symbols defined in Figure 2.
——— abscissa mean, ordinate mean
- - - - - - abscissa ±1std, ordinate ±1std
····· abscissa ±2std, ordinate ±2std

velocity angle is promising for the application of control systems to reduce the magnitude of vortices and downstream turbulence. This is because cross-correlations of the vortex magnitude between successive downstream regions **A**–**E** show the the vortices produced at the corner convect downstream. Figure 7(c) shows that a high level of vorticity at **A** is correlated with high levels of vorticity at stations **B**, **C** and **D** before the correlation peak reaches background noise levels at **E**. It is natural that such turbulent convection is accompanied by a decay in correlation peak, but this demonstrates a rationale for reducing vortex production, and hence noise and viscous drag, at the step to reduce levels throughout the whole downstream separation. Moreover, the results of Section 4.2 show that this could be achieved by addition of momentum in the upstream boundary layer.

5. Conclusions

The results of a high-speed and low-speed PIV experiments have been used to investigate and quantify the relation between various flow parameters. These parameters, defined in Section 3, were chosen to illuminate the mechanisms which govern the behaviour of the two separation regions of the flow over the forward-facing step.

It has been shown there exists a causal link between the upstream boundary layer and the flow over the step. The upstream wall shear stress correlates to the upstream extent of separation after a delay consistent with the average convection velocity of the lower boundary layer. Similarly, after an appropriate delay with respect to the upper boundary layer, the upstream displacement thickness correlates to the displacement thickness at the step.

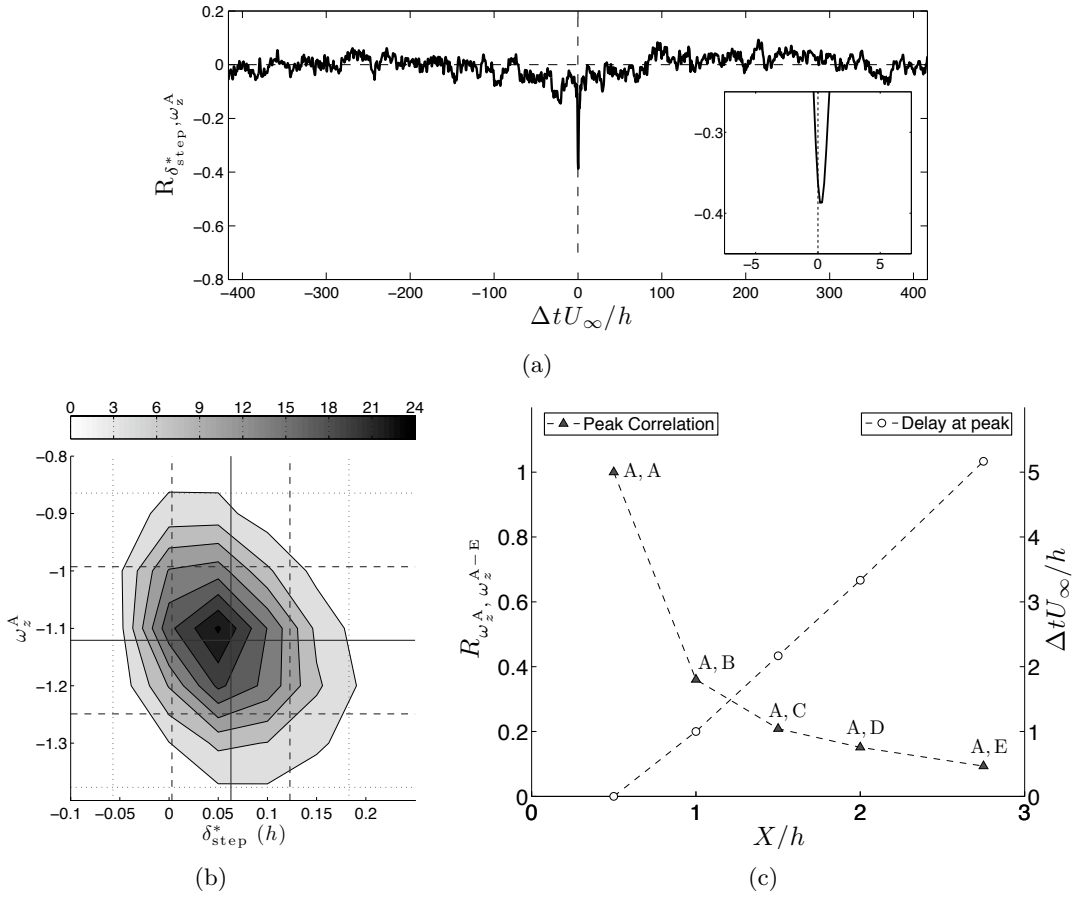

Figure 7. a) Cross correlation of δ^*_{step} and ω_z^{A}, b) the corresponding joint-pdf, c) Cross correlation peaks and time delays for the mean vorticity of regions **A** to **E**, referenced to **A**.

It has also been shown using joint probability density functions and cross-correlations, that a slower than average flow velocity above the step face is associated with an increase in the inclination of the flow above the step, an increase in downstream vorticity and an increase in the wall-normal extent of upstream reverse flow.

These results provide a basis for reducing the level of vorticity downstream of the step by appropriate addition of momentum to the upstream boundary layer. If successful, such a method would have implications for noise and drag reductions in numerous industrial applications.

Acknowledgments

The authors gratefully acknowledge Dantec Dynamics Ltd. for the loan of the high-speed PIV hardware and the EPSRC for grant number EP/F056206 which was used to purchase the low-speed PIV equipment.

References

Camussi, R., Felli, M., Pereira, F., Aloisio, G. & Di Marco, A. 2008 Statistical properties of wall pressure fluctuations over a forward-facing step. *Physics of Fluids* **20** (075113).

Kiya, M. & Sasaki, K. 1983 Structure of a turbulent separation bubble. *J. Fluid Mech.* **137**, 83–113.

Largeau, J. F & Moriniere, V. 2007 Wall pressure fluctuations and topology in separated flows over a forward-facing step. *Exp. Fluids* **42**, 21–40.

Sherry, M. J., Jacono, D. L., Sheridan, J., Mathis, R. & Marusic, I. 2009 Flow separation characterisation of a forward facing step immersed in a turbulent boundary layer. In *Sixth International Symposium on Turbulence and Shear Flow Phenomena*, pp. 1325–1330. Seoul, Korea.

Sigurdson, L. W. 1995 The structure and control of a turbulent reattaching flow. *J. Fluid Mech.* **298**, 139–165.

Stüer, H., Gyr, A. & Kinzelbach, W. 1999 Laminar separation on a forward facing step. *Eur. J. Mech. B/Fluids.* **18**, 675–692.